COSMIC Capstone Competition Technical Report

SCCRAM Jet

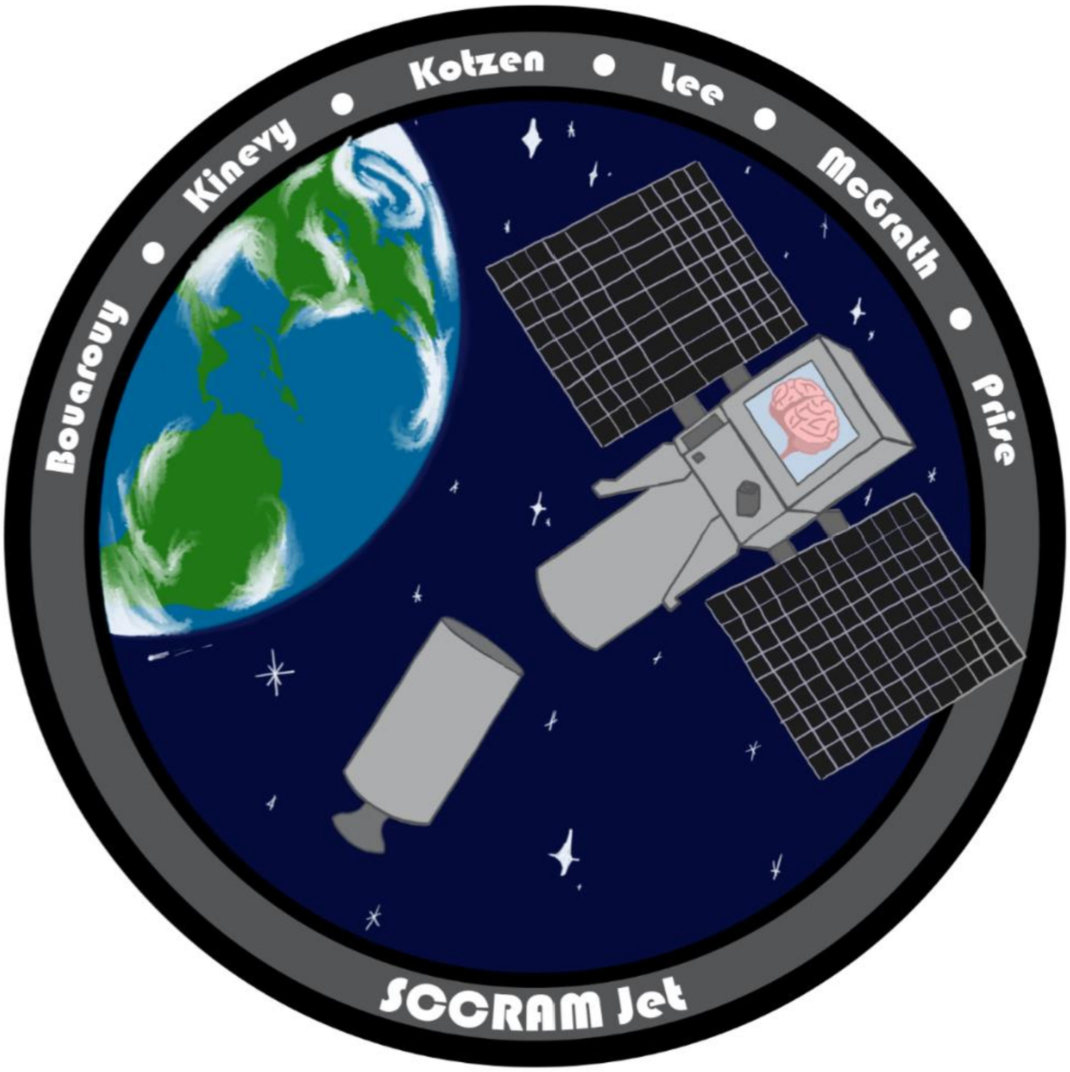

Christian Bouarouy, Maddy Kinevy, Sophia Kotzen, Coral Lee, Aidan McGrath, Ryan Prise

Instructor: Dr. Sara Lego, ses224@psu.edu

Mentor: Dr. Ed Tate, ed@virtussolis.space

April 10, 2025

Abstract
The SCCRAM Jet mission responds to the C3 Cosmic Capstone Competition's request for proposal (RFP) to design a spacecraft with autonomous servicing, assembly, or manufacturing capability [1]. Currently, satellites are often decommissioned due to a depletion of power from orbit limitations, component malfunctions, or diminishing battery capacity. The SCCRAM Jet team moved forward with a conceptual design of a payload that will resupply power by close-contact induction charging to inactive satellites, extending their lifespan. By extending the lifespan of decommissioned satellites, aerospace organizations can save time, money, and labor while simultaneously preventing unnecessary space debris with additional launches. Propulsion, structure, thermal, power, command and data handling, guidance navigation and control, and communication systems are thoroughly designed by requirements and systems engineering such that the SCCRAM Jet payload is integrated with the Blue Canyon Technologies (BCT) X-Sat Venus Class Bus for a successful mission. A risk mitigation decision matrix reflects risk reduction associated with each mitigation plan – responses to mission complications or failures. Future work involved in elevating the SCCRAM Jet mission to a preliminary design review (PDR) and further innovation in the aerospace industry are necessary to close vital technology gaps in the SCCRAM Jet mission architecture are outlined and discussed.

Introduction
Satellites often encounter challenges at the end of their lifespan with the diminishing ability of power generation, including orbit transfer, station-keeping, thermal regulation, and collision avoidance. So long as the power supply is maintained, a satellite may continue to function and carry out operations beyond its intended lifespan. Initial research into servicing satellites in orbit led to thorough research into satellite life extension. An example of servicing technology within Earth orbit is the Mission Robotic Vehicle (MRV) executed by NASA, with the goal of extending the lifespan of in-orbit satellites. The team learned that as long as power resupply, temperature regulation, and station-keeping are maintained, a satellite can continue to operate longer than its intended lifespan [2].

The status quo of satellite launching has become launching more satellites to replace those that lack power rather than recharging those satellites already in orbit. This pattern is due to the lack of reliable and cost-effective recharging technology in the spacecraft market. While technologies exist to repair physical failures on spacecrafts, such as the NASA MRV and Space Shuttle missions, these missions do not provide an autonomous method to refuel the electrical power system of a satellite [3]. The lack of efficient and proven in-orbit power resupply is a capability gap that the SCCRAM Jet payload aims to fill by using close-contact induction charging to repower a secondary cell battery of a dying target satellite.

Mission Overview
The goal of the SCCRAM Jet Mission is to resupply electrical power to a satellite with functioning components but diminished power supply. The main capability of the SCCRAM Jet payload will be to dock with other spacecraft in need of power resupply and utilize solar energy collected from onboard solar arrays to repower a target satellite. Repowering will allow the satellite to become fully operational and further extend the satellite's lifespan.

To resupply electrical power to a satellite in low Earth orbit, the SCCRAM Jet mission will feature a payload that rendezvouses with an existing target satellite and securely docks with the target satellite via a telescoping arm; the arm will feature a probe mass at its far end. Once the probe mass has been extended and secured into the target satellite's docking socket, the arm will retract and move the target satellite as close as possible to the payload. Using the power from the double solar arrays aboard the BCT X-Sat Venus Class Bus, the payload will convert solar power to electrical power; this power will be passed into the satellite's system via induction coils that will be placed at the far end of the payload itself as well as the face closest to the payload on the target satellite. This charging process is depicted in Figure 1. The act of reviving a satellite via induction charging in space has not been done before yet fills the necessary technology gap of spacecraft power resupply. The extending and retracting arm is also a novel way to dock, as almost all current docking arms are not retractable.

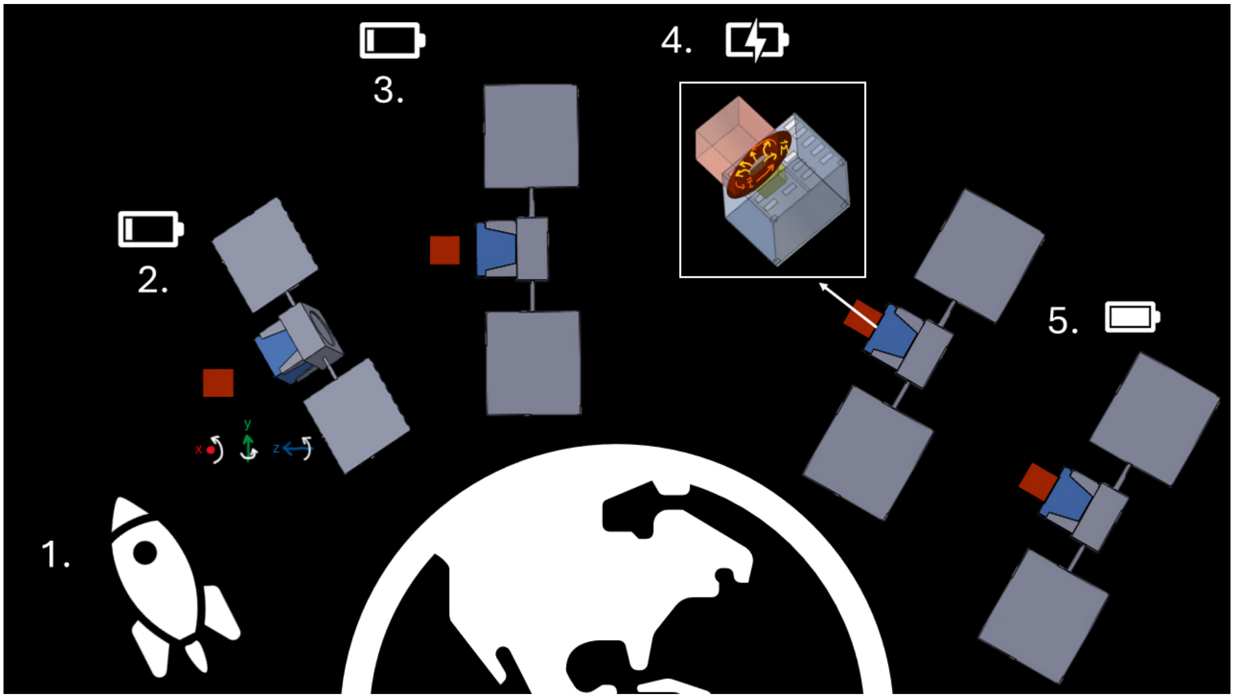

Figure 1. *SCCRAM Jet macro-level mission architecture.*

The SCCRAM Jet team established five top-level mission objectives that define the success of the mission. The objectives are as follows, with more details included in the team's System Requirements Review:

1. The payload shall demonstrate rendezvous capabilities with an existing satellite.
2. The payload shall demonstrate docking abilities with an existing satellite.
3. The payload must transfer power to an external satellite.
4. The payload will demonstrate ISAM capabilities while being hosted on the BCT X-Sat Venus Bus.
5. The payload shall demonstrate the ability to obey all national and international spacecraft laws and regulations.

Using the mission objectives as a guide for all necessary internal and external payload components, expected mass and power budgets were created for the SCCRAM Jet payload. These budgets include an additional 20% margin to account for any oversights in design. A bill of materials shown in Figure 2, and numerical values for both power and mass are listed in Figure 3.

PAYLOAD	
	Propulsion
	Holding thrusters (x8)
	Activaitng thrusters (x4)
	Gas N2 tank
	Plumbing
	Attitude Control
	Star trackers (x2)
	Sun sensor
	Power
	Induction coil
	Inverter (DC to AC)
	Rectifier (AC to DC)
	Secondary battery
	Wiring
	Structure
	Shell
	Levels (x4)
	Rods (x4)
	Screws (x8)
	Telescopic arm
	Thermal
	Louvers
	MLI covering
	Active Control Backup
	CDH
	On-board computer
	Wiring

BUS	
	Propulsion
	Hydrazine thrusters
	Power
	Primary battery
	Structure
	Aluminum alloy structure
	Thermal
	Radiators (active)
	Comms
	Antenna
	Software designed radio
	CDH
	On-board computer

Figure 2. *Bill of materials for SCCRAM Jet payload and BCT X-Sat Bus.*

Propulsion	11.3951	**Propulsion**	48.0000	**Propulsion**	0.1000
Attitude Control	0.1090	**Attitude Control**	0.4300	**Power**	22.2000
Power	3.5563	**Power**	172.2000	**Structure**	0.0000
Structure	7.9138	**Structure**	0.0000	**Thermal**	2.0000
Thermal	1.2164	**Thermal**	5.0000	**Comms**	5.8000
CDH	1.0100	**CDH**	1.2000	**CDH**	1.2000
		Subtotal	226.8300	***Subtotal***	31.3000
20% Margin	5.0401	**20% Margin**	51.6260		
TOTAL (kg)	30.2407	**TOTAL** (Watts)	309.7560		

Figure 3. *Mass budget for SCCRAM Jet payload & power budget for SCCRAM Jet mission.*

Payload Design

The servicing spacecraft will launch alongside the BCT X-Sat Venus Class Bus within the available volume. Once the payload establishes itself within the target satellite's orbit, the payload will align itself using the host vehicle's Guidance, Navigation and Control (GNC) system and begin nearing the target satellite. Once in close proximity to the target satellite, the payload will extend a telescoping arm with a probe mass at its end; this probe will enter the docking suite of the target satellite and be secured by the target satellite. The arm will then retract itself and pull the target satellite as close as possible to the payload, using a magnetic field induced the induction coil to extend and retract the telescopic arm. Once securely docked, power will begin to flow to the payload's induction coil and create an electromagnetic field surrounding the coil from the flowing voltage; this electromagnetic field will be received in the coil of the target satellite and induce a similar electric current that will ultimately be used to resupply charge to the target satellite's battery. A schematic of the rendezvous, docking, and induction charging process is detailed in Figure 4.

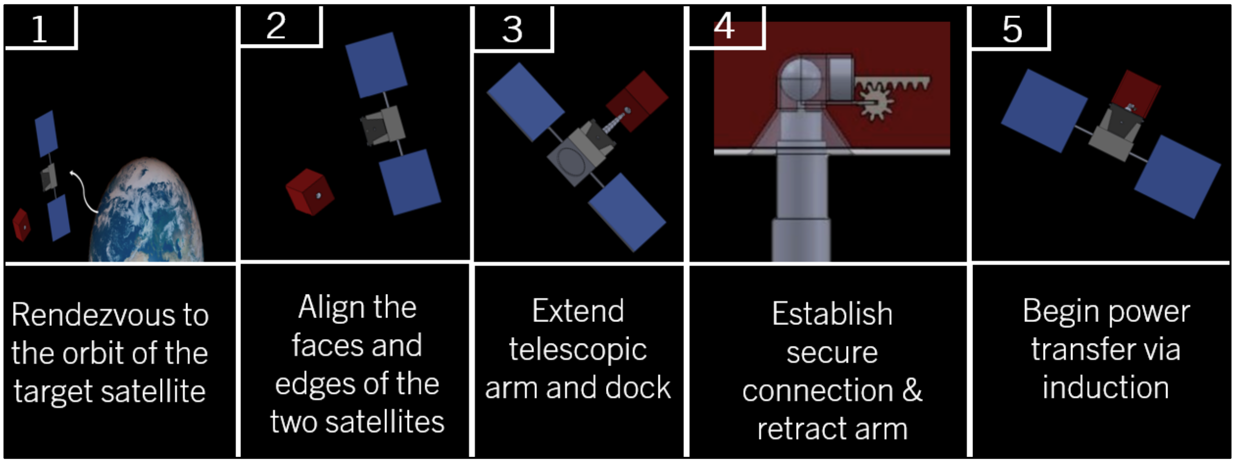

Figure 4. *SCCRAM Jet macro-level mission architecture.*

The SCCRAM Jet payload was designed by a bottom-up systems engineering approach. Design responsibilities were split into subsystems for equal workload and attention. The following section details the specifications of each payload subsections along with verification. Figure 4 outlines the finalized computer-aided design (CAD) model created using SOLIDWORKS. The model shown in Figure 5 features all components identified by each subsystem.

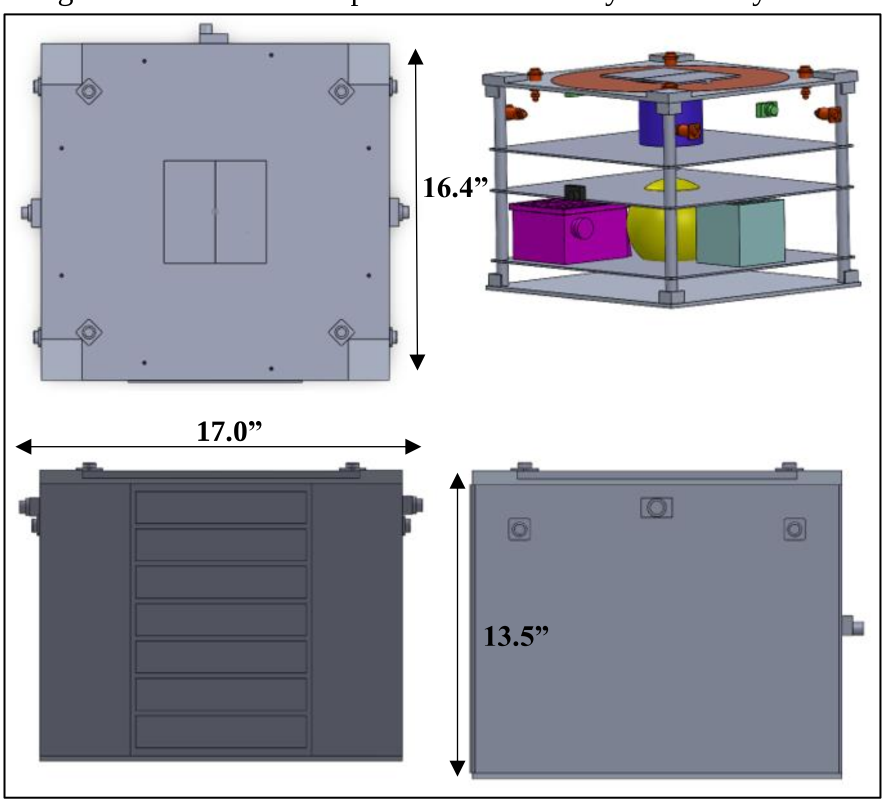

Figure 5. *Three-view of the SCCRAM Jet CAD model.*

Structures

The key responsibilities of the SCCRAM Jet payload structures subsystem were selecting suitable material and analyzing how this material would respond to mission operations. The mission required that the material be lightweight while maintaining a strong frame to hold components and simultaneously protect internals from space radiation and extreme temperatures. Through trade studies, the primary payload material selected was M60J, an aerospace grade high modulus carbon fiber [5]. With structural material selected, finite element analysis (FEA) was performed using SOLIDWORKS simulation on a simplified model to analyze how the material would perform under launch forces - the primary concern for structural failure. Results of the payload FEA are shown in Figures 6 and 7.

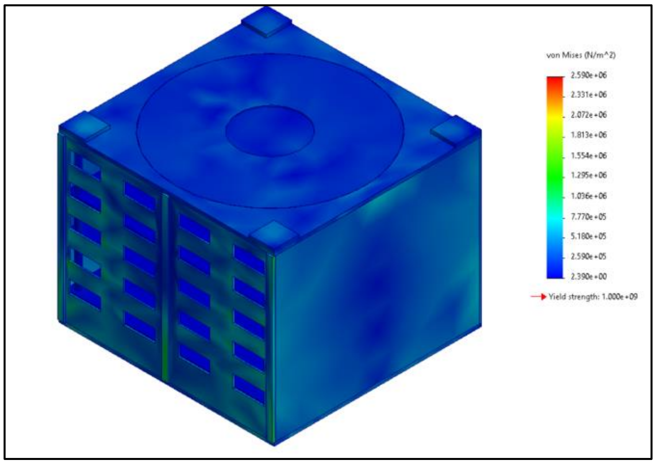

Figure 65. *Expected stress of payload (Pa).*

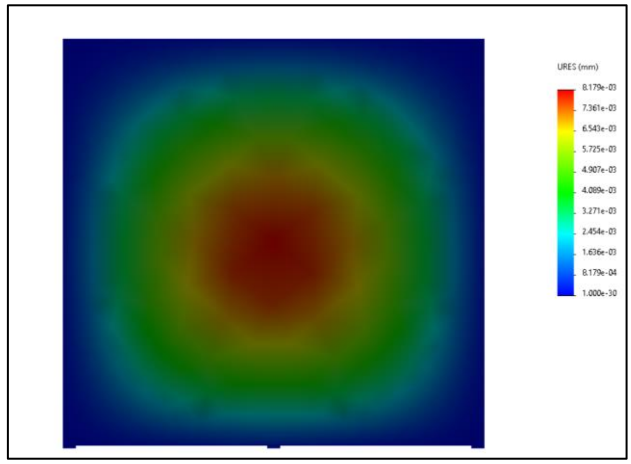

Figure 76. *Displacements on the payload's bottom plate (mm).*

Figures 6 and 7 were created by assuming that the payload would be held by four rails within the host spacecraft during launch. Rigid constraints were applied to the CAD model along the four side edges. The selected launch vehicle, the Electron Rocket, is specified to experience a maximum of 8 G's during launch; assuming a mass of approximately 30 kilograms, a force of roughly 2300 Newtons was applied, and the static simulation was run. The results showed that the majority of the stress is placed on the top and bottom plates during launch. Additional internal support rods were added within the frame and the thicknesses of these plates were doubled in the final CAD model to ensure mission success.

Power

The SCCRAM Jet team's payload will contain one B28-275 28-Volt Lithium-Ion Modular Battery; this selection was made by the given specifications of the BCT X-Sat Venus Bus in the RFP [1]. To transfer power between two batteries such that damage is avoided, they must have the same capacity and voltage [6]. Because the payload and bus batteries must have the same capacity, the payload battery must have the same capacity of 10.2 *Ah*. The B28-275 28-Volt Lithium-Ion Modular battery was the only battery with a capacity of 10.2 *Ah* that can withstand space environments.

The crux of the SCCRAM Jet mission is being able to transfer power via an induction coil within the payload. To determine the specifications of the coil itself, the design had to consider the RFP volume specifications, internal component locations, and amount of available power. The induction coil specifications are listed in Table 1.

Table 1. SCCRAM Jet induction coil design specifications.

SCCRAM Jet & BCT Bus Induction Coils [7]	
Outer Diameter	375.0 mm
Inner Diameter	100.0 mm
Wire Thickness	2.5 mm
Wire Cross-Sectional Area	4.9 mm^2
Number of Coil Turns	11
Total Length of Wire	8.2 m

With the coil geometry in Table 1, calculations determine the expected amount of power to be transferred to the target satellite. Power transfer calculations were performed assuming that the coil is made of copper, a material known for its high electric conductivity [8]. A total of 150 Watts is allotted to be sent to the coil for power transfer. With the power value and the known material constants of copper, the expected amount of current, resistance, and voltage within the induction coils of both the SCCRAM Jet payload and the target satellite are calculated by Ohm's Law and the resistivity equation. Coil specifications are summarized in Table 2.

Table 2. Electrical values during power transfer from SCCRAM Jet payload.

SCCRAM Jet Payload		Target Satellite	
Power to Coil	150.0 W	Voltage into Coil	1.23 V
Resistivity of Copper	$1.72 \bullet 10^{-8}$ Ω/m	Resistance in Coil	$2.88 \bullet 10^{-2}$ Ω
Resistance in Coil	$2.88 \bullet 10^{-2}$ Ω	Current in Coil	43.3 Amps
Voltage in Coil	2.08 V	Battery Capacitance	14.0 Ah

To simplify and standardize the induction charging process, values in Table 2 are calculated assuming the geometry of the payload and target satellite coils are identical. An transfer efficiency value of 60% was calculated, meaning that 60% of the voltage being passed to the target satellite is received by the target's coil [9]. The battery capacitance of 14 *Ah* was determined by estimating that the target satellite consists of 4 batteries, with each battery having a capacitance of 3.5 *Ah* - a standard for rechargeable lithium-ion batteries [10]. With the expected current within the target satellite's coil and a standard battery capacitance, the target satellite's battery can be recharged in just under 20 minutes; following this power resupply, the once decommissioned spacecraft can begin operations as normal and further extend its lifespan.

Propulsion

To select a propulsion system to integrate onto the SCCRAM Jet payload, first the thruster was chosen by trade study. Fourteen monopropellant, seventeen bipropellant, and four cold-gas thrusters – each having parameters characteristic to their design, were considered. Electric propulsion was initially considered, however lack of reliability and large engine mass deterred electric propulsion consideration for SCCRAM jet integration. Each thruster's technology readiness level (TRL), mass, length, propellant, nominal thrust, and specific impulse are considered as parameters. A trade study matrix was generated containing parameter information for all thrusters listed in the New Spacecraft Mission Analysis and Design textbook [11].

Quantified parameters of each engine: mass, length, nominal thrust, and specific impulse, are normalized in each category according to the function $n_i = \frac{v_i - v_{min}}{v_{max} - v_{min}}$, where v_i is the given engine's parameter, v_{min} is the minimum value of the parameter, and v_{max} is the maximum value of the parameter. As for status, all engines are well qualified for flight – meeting TRL 9. Propellant is judged by its ease of integration in respect to its insulation and pressure requirements. GN2 is the sole choice for all cold-gas thrusters and requires pressures of 150 to 2070 *kPa* with multi-layered insulation (MLI) blanket wrapping on propellant tanks for thermal protection [11]. Hydrazine is the sole propellant for all mono-propellant engines and can be operated with low temperatures and pressures. Bipropellants are beneficial in consideration of their high specific impulse; however, storage of fuel and oxidizer is cumbersome and requires complex pressurizing mechanisms. Considering the complexity involved with bipropellant storage, thruster trade study progressed only with monopropellant and cold gas options.

Monopropellant thruster engine lengths range anywhere from 3.94 to 16.18 inches - which would encroach on space dedicated to SCCRAM Jet internal mechanisms. Cold gas thrusters are desirable in every parameter except specific impulse. However, specific impulse is not necessarily a priority for the SCCRAM Jet propulsion suite – which will solely handle attitude control and docking adjustments. Proceeding with the thruster trade study, three cold gas thrusters are left as viable options for the SCCRAM Jet propulsion system. See Table 3 for a normalized cold-gas thruster trade study matrix, where parameter normalizations are generated such that when higher parameters are undesirable, the normalization function then follows $n_i = 1 - \frac{v_i - v_{min}}{v_{max} - v_{min}}$ so that a high undesirable value is 0 and a low desirable value is 1.

Table 3. *Normalized cold-gas thruster system trade study matrix.*

ENGINE	ENGINE MASS	LENGTH	THRUST	I_{sp}	OPERATING PRESSURE
SVT01 Solenoid Valve Thruster	0	1	0	0.852459016	1
Solenoid Actuated 58E142A Thruster	1	0	0.031518625	0	0.857357357
Solenoid Actuated 58-118 Thruster	0.828571429	0.618181818	1	1	0

High undesirable parameters in the thruster trade study include engine mass, length, and operating pressure. A high operating pressure corresponds to a stronger fuel tank, and therefore more mass – as does a large engine mass. A longer engine is undesirable in respect to the conservation of room for SCCRAM Jet internal mechanisms. A high thrust and high I_{sp} correspond to a more powerful and fuel-efficient engine, respectively.

Observing Table 3, there is not a clear engine which excels in all parameters. Each parameter is weighted according to its importance to the SCCRAM Jet mission. Engine mass receives a 10% weightage, since all cold-gas engines listed are reasonably negligible compared to the 70 *kg* constraint. Thruster length is a 40% weightage, due to the importance of conserving internal space in the SCCRAM Jet payload volume. Thrust is weighted at 5%, because all thrusters are relatively close to each other in thrust performance, and long burns are expected for attitude control. Specific Impulse is scored at 20%, for the energy-to-mass efficiency of on-board propellant is essential to mass budgeting. In a similar regard, operating pressure is weighted a 25% importance, as it directly dictates the mass of the fuel container for the thrusters.

Total engine desirability based on weightages is calculated by $desirability = \sum weight_i * n_i$, where i represents each parameter. Calculating the desirability for each thruster, the SVT01

Solenoid Valve Thruster scores a 0.820, the Solenoid Actuated 58E142A Thruster scores a 0.316, and the Solenoid Actuated 58E118 Thruster scores a 0.580 – meaning the SVT01 Solenoid Valve Thruster is the best thruster for the SCCRAM Jet propulsion system.

Thruster locations must be determined before impulse calculations are made. It is assumed that the BCT Bus can be modified such that thrusters may be placed on its exterior for attitude control. The SVT01 Solenoid Valve Thruster has a variable thrust range of 0.1 to 1 *N*, meaning thrusters may be placed at different moment arms and still generate equal moments about the rotation axis, as long as their thrust is adjusted accordingly. To reduce plumbing complexity and foster a simple design, a total of 12 SVT01 Solenoid Valve thrusters are integrated on the SCRAMM Jet and Bus satellite – offering 3-axis attitude control. Thrusters are placed so that their impulse maximizes their moments imparted upon the SCCRAM Jet & Bus satellite.

Next, the size and mass of the gaseous Nitrogen tank is calculated by adding the total thruster firing time expected for all ΔV maneuvers during the SCCRAM Jet mission, and solving for the required pressure and mass of gaseous Nitrogen required. A sequence of 5 ΔV maneuvers is expected for the SCCRAM Jet mission: translational zeroing, °180 spins about the smallest and second smallest moments of inertia, docking, and spin-up of the docked assembly. Aided with CAD models of the SCCRAM Jet assembly and a target satellite modeled after a Landsat observatory, moments of inertia are calculated for each. Linear and rotational kinematic equations are used to calculate the total thruster firing time to be 138.95 *s*. The mass flow rate of the SVT01 Solenoid Valve thrusters is given by the equation $\dot{m} = \frac{thrust}{\mathrm{I_{sp}} * g_0}$, where thrust is equal to 0.1 Newtons and $\mathrm{I_{sp}}$ is 72 *s*, resulting in $\dot{m}$ = 0.00014 $\frac{kg}{s}$. Total thruster firing time is multiplied to find the total propellant mass. Assuming the stored gaseous nitrogen behaves as a perfect gas, the propellant tank weighs 6.78 *kg*, given the hoop stress resulting from a 1 *cm* thick spherical Aluminum tank with radius 13.6 *cm* is equal to the 150 *kPa* operating pressure of the SVT01 Solenoid Valve thruster – well below Aluminum's 110 *MPa* yield strength.

Thermal

The temperature range found to be most optimal for all on-board sensors was $-10^{o}C$ to $50^{o}C$ [12]. To find the ideal thermal ventilation system for the SCCRAM Jet payload, a trade study was conducted between two reliable and proven operations shown in Table 4. Deployable radiators and passive louvers offer proven solutions to dissipate the buildup of thermal radiation within a spacecraft.

Table 4. *Thermal analysis for SCCRAM Jet payload design.*

Characteristics	Louver System	Deployable Radiators
Complexity	Passive, operates with bimetallic springs which expand and contract based on the internal temperature of the payload wall, will be built directly as a part of payload	Passive, requires deployment, one of the payload faces will have to be a radiator
Reliability	Operate based on thermodynamic principles and entropy, could encounter issues with sudden temperature changes i.e eclipses	Max heat loss: 2.75 W at 90deg, will continue to dissipate heat at a constant level, can reduce internal temperatures by around 50 C with the proper rotation
Efficiency	Responds to the internal payload temperature, could have interference when inside bus	Can be actively rotated, changing the total amount of heat dissipation but requires a 135-degree rotation to achieve "full deployment", will continually radiate given amount based on sunlight exposure
Power Consumption	Will not require power, some heat WILL be absorbed into the bimetallic springs which will need to be	Requires power (around 2.5W) for deployment and panel rotation

	accounted for to properly dissipate heat ->backup will be installed additionally	
Volume Budgeting	Will be attached directly the payload, must create internal space within the payload for the louvers to fit	Will fit on the payload externally, probably along the bottom of the payload to fit inside the bus
Mass Budgeting	Aim for around 8 kg/m^2, need space for multiple flaps to properly dissipate heat but will be a part of the payload itself	Extra pieces required in addition to the full mass of the payload, 0.5 kg per panel (4 panels needed to keep the center of mass stable) meaning that around 2 additional kgs on top of the full mass of the payload will be needed
Dissipation Properties	Dissipates heat directly through the louver flaps, could run into issues when conducting control volume analysis	Vent system can be pointed towards deep space to release heat, easily removing excess heat from the system
Results	**Best Fit for Payload Thermal Design**	**Non-Ideal Option for Payload Thermal Design**

Characteristics such as volume, mass, power consumption, and efficiency were heavily considered in the formulation of this trade study. Ultimately, the passive louver system offered more budgeted mass and volume constraints as well as a reduced amount of power consumed. With the passive louver system, bimetallic springs are connected to louver "blades" which effectively emit heat. Thermal radiation is absorbed by the bimetallic springs, causing them to expand due to the difference in thermal coefficients between the two fused metals. The blades themselves change angle based on the expansion of the springs. The change of angle for these blades allows for a higher emissivity factor, designed to emit a larger amount of heat when opened at a larger angle. Ultimately, using a 7-blade single row louver system, each blade will have an effective emissivity of 0.14 combining for a total emissivity of about 0.75. A radiator mounting surface will be attached to the louver system against the payload surface with an emissivity of 0.85 [12].

Around 40% of the power used by the induction coil (150 Watts) will be lost to heat dissipation as well as thermal radiation from the battery (22.2 Watts) and miniscule amounts of heat radiated from onboard sensors. A total of about 70.4 W of power will be dissipated as heat. Using the Stefan-Boltzmann Law to describe the heat radiation within the system, $Q = \sigma \varepsilon A T^4$, it can be calculated that the temperature on the external surface of the payload will be about 46.85°C (320 K). External surface temperature falls within the acceptable temperature range for the passive system to effectively emit heat, but does reside in the upper quartile. To ensure redundancy, an active control backup to manually control the louver system will be paired with thermocouple probes, measuring the temperature along the surface wall of the craft. If an unexpected event, such as an eclipse, is to occur and the payload falls out of its established temperature range, the active control system will be used to manually achieve the desired angle for the louver blades - drawing around 5 W of power.

The exterior of the payload will be lined with a multi layered insulation (MLI) blanket to absorb incoming solar radiation. The exterior MLI blanket will be black Kapton laminate, which is specifically designed for the exterior of spacecraft, operates between temperatures of –200 to 400°C, and has an area to emissivity ratio of 1.10 (very effective). Around 95 to 100% of the incoming solar radiation will be reflected by this material before affecting the internals of the craft [13]. Internally, the plumbing and propulsion tank will be wrapped in lightweight aluminized polyester film - an MLI blanket designed for internal components. Aluminized polyester film has a large operating range, like black Kapton laminate, and will provide extra individual protection for these components - ensuring thermal redundancy on top of the louver system in place.

Command & Data Handling (C&DH)

The payload will operate on a backplane integration and configuration of four computer systems: main, payload, power, and attitude/orbit. Figure 8 shows a flowchart of the communications between each computer system, with payload and power communicating regularly with one another as power and the payload are linked closely together.

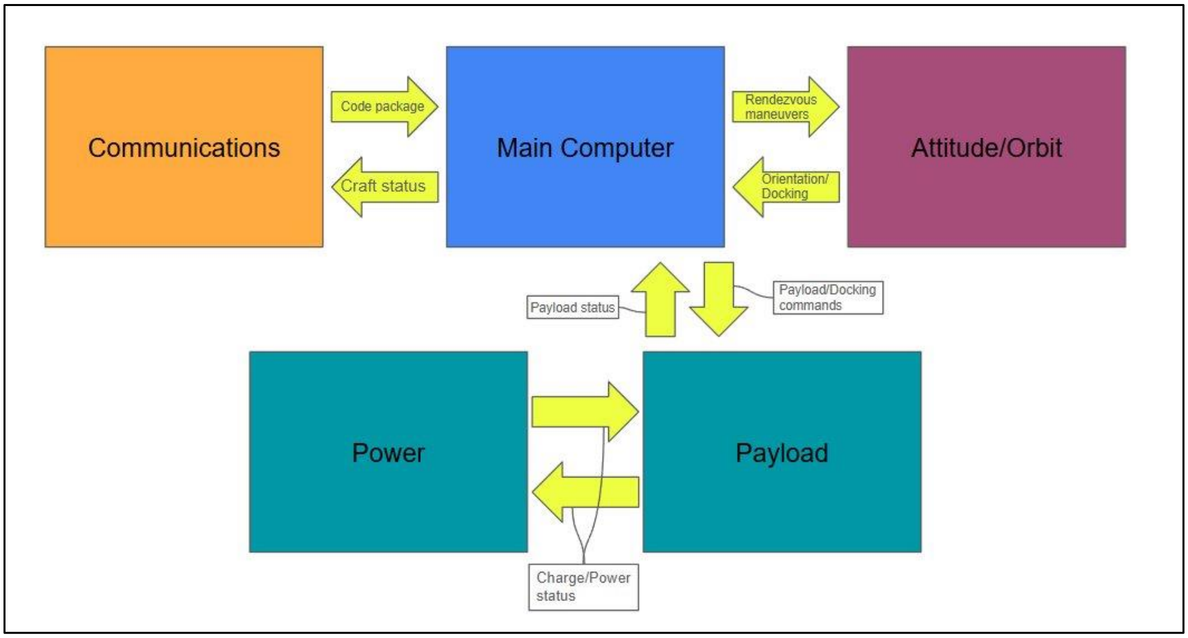

Figure 87. *C&DH flowchart by Christian Bouarouy.*

A trade study shown in Table 5 shows backplane in comparison to PC-104, with backplane best fitting the needs of the mission.

Table 5. *C&DH integration trade study.*

Criterion	PC-104	Backplane
Size	Compact in size due to configuration standardization	Larger size to accommodate adaptable integration
Weight	Lightweight due to compact configuration	More weight due to larger configuration
Power Draw	Power distribution across individual components constrained due to small size configuration	Centralized power distribution across components
Signal Integrity	Constrained bandwidth and lower signal integrity	High bandwidth and better signal integrity
Expandability/Flexibility	Stack height limitations and rigid modularity	Flexible configuration and able to be expanded due to larger configuration size
Cost	Lower component and configuration cost	Higher component and configuration cost
Complexity	Standardized and modular design	Higher complexity due to flexible configuration
Overall Performance	Limited in performance due to size, power, and bandwidth constraints	Increased performance based on power distribution, flexibility, and better signal integrity
Results	**3**	**5**

C&DH subsystem will be capable of a peak data transfer rate of 1.92 *Mbps* with an average download speed of 1 *Mbps* and an average upload speed of .96 *Mbps* [14]. The C&DH configuration will utilize field programmable gate arrays (FPGAs) and magnetometers (MAGs) to efficiently capture, store, and transfer the various data collected with the ability to carry out differing commands based on mission requirements. The C&DH configuration for the payload is estimated to be 1 *kg* in mass and roughly 1U (10*cm* x 10*cm* x 10*cm*) in size. Average power consumption is estimated to be 1.2*W* with a peak of 4.7*W* and featuring a centralized power distribution via the backplane to each of the four computers [15].

Host Spacecraft Integration & Mission Analysis

Integrating the SCCRAM Jet payload into the BCT X-Sat Venus Class Bus required that all assumed or modified subsystems within the bus be verified. The following section details each subsystem of the bus and what work was done to confirm or alter its components.

Structures

Because the specific material used by BCT to manufacture the bus is unknown, assumptions had to be made to complete further analysis. After general spacecraft research, it was found that aluminum alloys, specifically 6061, are extremely common in the satellite industry. Using a metal procurement standards document found on the BCT website, it was confirmed that BCT uses aluminum alloy 6061 in their manufacturing, although not for which products [16]. The outer shell is assumed to be approximately 5 *mm*, considering that CubeSats are usually 1-2 *mm* thick, and the bus is roughly twice the size of a standard CubeSat [17].

To verify that the presumed bus structure is valid, a simplified load analysis was performed via SOLIDWORKS Simulation. The Electron Rocket is expected to experience a maximum of 8 G’s during launch; this load value was applied to a CAD model of the bus with a material of aluminum alloy 6061 which has a maximum yield load of 83 *MPa* [18, 19]. Approximations of the bus’s dimensions were made by pixel measurement comparison with known physical dimensions. The only known physical dimension of the BCT X-Sat Venus Bus is its 15” ESPA ring, the payload adapter for securing the bus during launch [20]. After running the simulation, the maximum expected stress within the bus frame was less than the yield strength of aluminum 6061, confirming the validity of the aluminum 6061 frame.

Power

The RFP states that the bus will have either single solar array panels with an available power of 222 *W*, or dual solar array panels with an available power of 444 *W* [1]. The SCCRAM Jet team determined using dual solar arrays would be best so that there would be more available power to use throughout the bus and the payload. The SCCRAM Jet mission is to resupply power to satellites, so having more available power is crucial.

The dual solar panels have 30% efficient solar cells, a honeycomb structure with carbon fiber substrates, and an array voltage of 36.2 *V* (DC) according to the information provided by BCT [20]. Having 30% efficient solar cells means only 30% of the sunlight that is shined on the solar cells is converted into electrical energy; 70% of sunlight is not converted. Further research showed that the solar cell is photovoltaic which, by definition, means that the solar cells convert sunlight to electrical energy [21].

Table 21-13 in the SMAD textbook provides different types of solar cells along with their efficiencies. Information provided in this table along with the fact that the solar cells are 30%

efficient as stated by BCT shows they are Triple Junction GaAs [22]. There is constant power generation through the solar panels because the bus and payload will be in an SSO, meaning they will always be facing the sun, therefore always receiving sunlight to convert to electrical energy.

Another constraint the RFP specifies is that the Bus can store up to 10.2 *Ah* of energy. Through extensive research, it was determined that the battery used for the bus is a B28-275 28-Volt Lithium-Ion Modular Battery. A B28-275 28-Volt Lithium-Ion Modular Battery is assumed to be the battery used for the Bus because of the estimated bus dimensions constraints, energy storage capacity of 10.2 *Ah*, and its survivability in space environments.

Internal components that require power belong to the propulsion, C&DH, COMMS, GNC, and thermal subsystems. In addition, power must be transferred to the battery contained within the payload. According to the power budget provided in Figure 3, the power required for the internal components of the Bus is 31.3 *W*, leaving 412.7 *W* of power to transfer to the payload battery.

Thermal

Using a similar trade study as with the thermal subsystem for the payload, it was found that deployable radiators are the best choice to emit heat from the bus. Key differences include the volumetric constraints of the bus which, in turn, affect the complexity of the radiator system. Given that less equipment will be contained within the bus, it is easier to devote more payload volume to becoming a part of the radiator system. This was the biggest issue with the payload, as sensors and a large battery are contained within.

The deployable radiators are used to maintain strict temperature controls on electronics and other instruments. Radiators used will be 365 x 82 x 20 *mm* and will have a weight of 8 $\frac{kg}{m^2}$ [23]. Leading to a total mass of 0.24 kg for the entire radiator system. To fully deploy, the radiators must be rotated 135° from their starting position. Maximum heat dissipated by the system will occur at a 90° angle of deployment offering a 2.75 *W* dissipation. At max emission, deployable radiators can reduce the internal temperature of the bus spacecraft by 50°C [24].

Command & Data Handling (C&DH)

Due to the unknown specifications of the bus, it is assumed that the bus and the payload will be operating on the same C&DH subsystem with the same specifications. A unified C&DH system is assumed because of the relative simplicity of the commands to reduce power draw, unnecessary redundancies, points of failure, and overall cost.

Host Spacecraft Integration & Mission Analysis

Part of designing the SCCRAM Jet payload is ensuring that the payload's components successfully interface with the BCT X-Sat Venus Class Bus. The following section details the designated systems within the bus and how the SCCRAM Jet team verified each of the host spacecraft's subsystems.

Ground System

The SCCRAM Jet mission will utilize the onboard communications system of the BCT X-Sat Venus Class Bus, as detailed in this section. As depicted in Figure 9, the mission employs a low-altitude, single-satellite, store-and-forward architecture for data transmission within the S-band frequency.

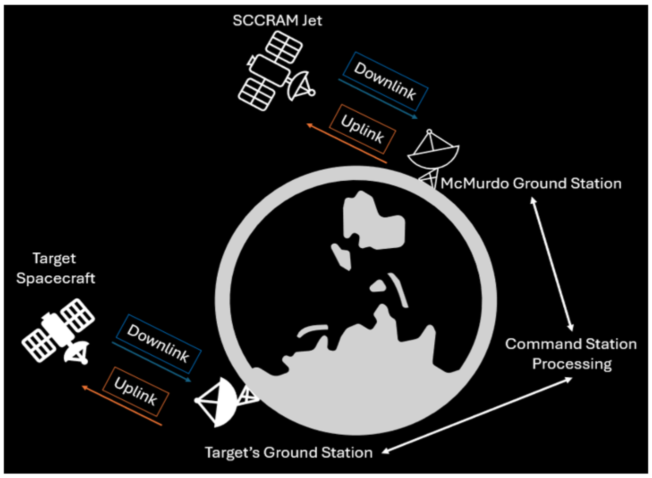

Figure 98. *Communication architecture schematic for SCCRAM Jet Mission.*

Due to the mission's polar orbit, ground station selection prioritized locations at latitudes closest to Earth's poles, along with the availability of transmitter (Xmtr.) data [25]. The trade study evaluated candidate ground stations based on orbit compatibility, transmitter power, antenna diameter, and logistical complexity, as summarized in Table 6. Green indicates the best ranking, red is the lowest, and orange denotes moderate favorability.

Table 66. *Ground station qualitative decision matrix.*

Characteristic	McMurdo G.S	O'Higgins G.S	Trollsat G.S.
Xmtr. Power (W)	200.0	0.2	N/A
Xmtr. Ant. Diameter (m)	10.0	9.0	7.3
Latitude	-77.81	-63.32	-72.10
International Cooperation (Logistic Complexity)	No	Yes	Yes

The transmitter power for the O'Higgins ground station is derived from the European Remote Sensing Satellite, which utilizes O'Higgins as its ground station [26]. O'Higgins transmitter power value may not represent the station's full capabilities but is the only publicly available confirmed figure. As displayed in Table 6, the McMurdo ground station is most compatible with mission requirements while also having the greatest capabilities.

Tables 7 and 8 present the uplink and downlink link budgets for communication between the McMurdo Ground Station and the SCCRAM Jet spacecraft. These link budgets follow templates from Professor Sara Lego's Aerospace 401B Capstone Course at Penn State. Green cells indicate values input by SCCRAM Jet. Grey cells indicate values input or calculated by the template. In the source column, the references and equations are from Chapter 13 of SMAD 3rd Edition.

Table 7. *Uplink link budget for SCCRAM Jet mission.*

Value Name	Symbol	Units	Source	Value
Freq.	f	Ghz	S-band frequency	**2.00**
Xmtr Pwr	P	W.	McMurdo Value	**200.0000**
Xmtr Pwr	P	dbW	10 log(P)	23.01
Xmtr line loss	L_l	dB	Standard Estimate	**-1.00**
Xmtr Ant. Beamwidth	θ_t	deg	$21 / (f \bullet D_t)$	1.050
Peak Xmt. Ant. Gain	G_{pt}	dB	$44.3 – 10\log_{10}(\theta_t^2)$	43.88
Xmt. Ant. Diam.	D_t	m	McMurdo Value	**10.00**
Xmt. Ant. Pointing Error	e_t	deg	Standard Estimate	**1.00**
Xmt. Ant. Pointing Loss	L_{pt}	dB	$-12 \bullet (e_t/\theta_t)^2$	-10.88
Xmt Ant. Gain	G_t	dB	$G_{pt}+L_{pt}$	32.99
EIRP	EIRP	dB	$P+L_l+G_t$	55.00
Prop. Path Length	S	km	Orbital Subsytem + G.S. Alt.	**5.002E+02**
Space Loss	L_s	dB	$20\log_{10}(3\bullet10^8)-20\log_{10}(4\pi)-20\log_{10}(S\bullet10^3)-20\log_{10}(f\bullet10^9)$	-152.44
Prop. & Polariz. Loss	L_a	dB	Fig. 13-10	**0.01**
Rcv. Ant. Diam.	D_r	m	S-band patch antenna	**0.08**
Peak Rcv. Ant. Gain	G_{rp}	dB	$-159.59 + 20\log_{10}(D_r) + 20\log_{10}(f\bullet10^9) + 10\log_{10}(0.55)$	1.47
Rcv. Ant. Beamwidth	q_r	deg	$21 / (f \bullet D_r)$	137.80
Rcv. Ant. Pointing Error	e_r	deg	Standard Value	**0.05**
Rcv. Ant. Pointing Loss	L_{pr}	dB	$-12(e_r / \theta_r)^2$	0.00
Rcv. Ant. Gain	G_r	dB	$G_{rp}+L_{pr}$	1.47
System Noise Temp.	T_s	K	Table 13-10	**614.00**
Data Rate	R	bps	C&DH Subsytem	**1920000.00**
Est. E_b/N_o (1)	E_b/N_o	dB	$EIRP + L_s + L_a + G_r + 228.6 – 10\log_{10}(T_s) – 10\log_{10}(R)$	41.93
Bit Error Rate	BER	--	Reed Solomon Channel Coding	**1.0E-05**
Rqd. E_b/N_o (2)		dB	Fig. 13-9 (BPSK, R-1/2 Viterbi)	**2.50**
Implementation Loss (3)	L_i	dB	Standard Estimate	**-2.00**
Margin		***dB***	***(1)-(2)+(3)***	***37.43***

A key consideration in this analysis is the selection of values from a given range to minimize link margin, ensuring the margin is not overestimated. For instance, while a 0.96 Mbps data rate is expected, the 1.92 Mbps maximum value was used to provide a conservative estimate. Despite the conservative estimate, the link margin is significantly higher than the recommended 20 dB for commands and 3dB for data. This is due to the large diameter and high power of the McMurdo ground station antenna.

Table 8. Downlink link budget for SCCRAM Jet mission.

Value Name	Symbol	Units	Source	Value
Freq.	f	Ghz	S-Band Frequency	**2.00**
Xmtr Pwr	P	W.	S-band Patch Antenna	**4.0000**
Xmtr Pwr	P	dbW	10 log(P)	6.02
Xmtr line loss	L_l	dB	input	**-1.00**
Xmtr Ant. Beamwidth	q_t	deg	$21 / (f \bullet D_t)$	137.795
Peak Xmt. Ant. Gain	G_{pt}	dB	$44.3 – 10\log_{10}(\theta_t^2)$	1.52
Xmt. Ant. Diam.	D_t	m	80mm X 80mm	**0.08**
Xmt. Ant. Pointing Error	e_t	deg	Standard Value	**1.00**
Xmt. Ant. Pointing Loss	L_{pt}	dB	$-12 \bullet (e_t/\theta_t)^2$	0.00
Xmt Ant. Gain	G_t	dB	$G_{pt}+L_{pt}$	1.51
EIRP	EIRP	dB	$P+L_l+G_t$	6.54
Prop. Path Length	S	km	Orbital Mech. + G.S. Alt.	**5.002E+02**
Space Loss	L_s	dB	$20\log_{10}(3\bullet10^8)-20\log_{10}(4\pi)-20\log_{10}(S\bullet10^3)-20\log_{10}(f\bullet10^9)$	-152.44
Prop. & Polariz. Loss	L_a	dB	Fig. 13-10	**0.01**
Rcv. Ant. Diam.	D_r	m	McMurdo Value	**10.00**
Peak Rcv. Ant. Gain	G_{rp}	dB	$-159.59 + 20\log_{10}(D_r) + 20\log_{10}(f\bullet10^9) + 10\log_{10}(0.55)$	43.83
Rcv. Ant. Beamwidth	q_r	deg	$21 / (f \bullet D_r)$	1.05
Rcv. Ant. Pointing Error	e_r	deg	Standard Value	**0.05**
Rcv. Ant. Pointing Loss	L_{pr}	dB	$-12(e_r / \theta_r)^2$	-0.03
Rcv. Ant. Gain	G_r	dB	$G_{rp}+L_{pr}$	43.81
System Noise Temp.	T_s	K	Table 13-10	**135.00**
Data Rate	R	bps	C&DH Subsytem	**1000000.00**
Est. E_b/N_o (1)	E_b/N_o	dB	$EIRP + L_s + L_a + G_r + 228.6 – 10\log_{10}(T_s) – 10\log_{10}(R)$	45.20
Bit Error Rate	BER	--	Reed Solomon Channel Coding	**1.0E-05**
Rqd. E_b/N_o (2)		dB	Fig. 13-9 (BPSK, R-1/2 Viterbi)	**2.50**
Implementation Loss (3)	L_i	dB	Standard Estimate	**-2.00**
Margin		***dB***	***(1)-(2)+(3)***	***40.70***

Similarly to the uplink, the downlink margin greatly exceeds the required value due to the McMurdo Ground Station’s antenna size. An exceeding downlink margin ensures reliable communication throughout the mission.

Launch Vehicle

In a trade study among the SpaceX Falcon 9, Ariane 6, Polar Satellite Launch Vehicle, and Northrop Grumman Minotaur-C, Rocket Lab’s Electron Rocket was chosen to launch the SCCRAM Jet mission. Electron’s wide range for mass and volume capacities, adjustability for orbital altitude placement, low load factor during launch, cheap cost of $5.7 million, and 93.3% success rate made it a clear choice for the mission launch vehicle over its competitors. [18]

Orbit Selection

Selection of the orbit for the SCCRAM Jet mission was motivated by ability for solar array generation, launch vehicle capability, and occupation of power-degraded satellites. To reach said orbit, SCRAMM Jet must abide by the ΔV capability of the Electron rocket. For mission operations, frequent ground station contact is necessary. SCCRAM Jet's last orbital constraint is that the orbit must host satellites that could benefit from a SCCRAM Jet payload servicing. A sun-synchronous orbit (SSO) happens to satisfy all SCCRAM Jet orbit constraints. With an uneclipsed view of the sun and need of only 1 ground station, Landsat observatories also occupy a SSO and decommission due to lack of power supply [27].

Risks & Fault Recovery

As with any spacecraft, the SCCRAM Jet mission comes with risks, some more severe than others. Table 9 details the five most pertinent risks with the current mission architecture.

Table 9. *SCCRAM Jet mission risks.*

Risk		Pre-Mitigation	Mitigation Strategy
Docking	1. Docking arm connection	Docking with target satellite will affect the COM of the system therefore changing orbital mechanics and orbit.	Propellant reserve for additional ΔV.
	2. Docking arm extension	Docking arm may not extend due to a magnetic repulsion.	Spin satellite to induce a radial acceleration of telescopic arm.
Power	3. Induction coil EM field	Inducing an EM field between the satellites could infer with existing/unprotected internals.	Ensure high magnetic permeability materials in the target satellite.
	4. Distance between coils	The target satellite's coil may not be within a few millimeters of the payload, preventing efficient power transfer.	Explore using resonant inductive coupling.
Thermal	5. Eclipses and solar flares	Unexpected changes in temperatures can push components to inoperable ranges.	Incorporate active control backup for louver system.

The SCCRAM Jet team proposed potential mitigation strategies for each of the five key risks which are listed in the last column of Table 9. These mitigation strategies are designed for further implementation in the case the SCCRAM Jet mission would move forward in the design process. Table 10 is a risk analysis matrix that ranks each risk on a scale from high to low for both probability and overall mission impact. The risk analysis matrix shows that most of the mission's risks are categorized near the moderate and significant impact level with possible probability. Mitigation strategies for each risk move all risks to the "watch" or "acceptable" category, demonstrated by the arrows connecting numbers corresponding to each risk in Table 9.

Table 10. *Risk analysis & mitigation matrix.*

Probability						
	Very Likely					
	Likely					
	Possible			4	2, 3	5
	Unlikely			4	1, 2, 3	
	Very Unlikely				1	5
		Negligible	Minor	Moderate	Significant	Severe
		Impact				

Risk Level	Acceptable	Watch	Unacceptable

Future Work

While significant progress was made in designing and analyzing the SCCRAM Jet payload and the host spacecraft verification, there is still plenty of work to complete before a SCCRAM Jet mission is ready for launch. Table 11 details the future work that needs performed if the mission were to be advanced, broken down by subsystem.

Table 11. *Future work for the SCCRAM Jet mission.*

	SCCRAM Jet Payload	BCT X-Sat Venus Class Bus
Structures	Additional FEA analysis with all CAD internals	Research into in-orbit torque(s) on solar arrays
Power	Improving coil efficiency, real-life power transfer verification	Confirmation of dual solar arrays and battery details
Thermal	Thermal Analysis using CAD software, Risk Scenario Thermal Analysis	Thermal Analysis using CAD Software
Propulsion	ADCS Design, Docking Simulation	Confirmation of Thruster placement, ADCS Design, Docking Simulation
C&DH	OpenC3 Cosmos application analysis	OpenC3 Cosmos application analysis

Future work on improving battery power and energy density will allow for more energy to be stored and less energy lost during power transfer and discharge in a smaller, lighter battery. Work to improve battery power and energy density includes researching, discovering, and developing smaller, lighter active materials, researching more efficient ways to package the cells, and increasing the percentage of active to inactive materials. Increased discharge rate allows for quicker power delivery, meaning less docking time in terms of the SCCRAM Jet team’s mission. Currently increasing discharge rate means reducing longevity. Future work involves determining how to increase discharge rate, while also increasing longevity [28].

A compact, low-weight electric thruster would improve the specific impulse of the payload propulsion system - enabling a SCRAMM Jet assembly to service multiple satellites per mission. Developing a smaller, more reliable electric propulsion engine would fill this technological gap.

Global adoption of a universal docking suite for small satellites would be advantageous, for the range of satellites a SCRAMM Jet mission could service would broaden – as opposed to the custom target satellite docking suite designed by the SCRAMM Jet team.

References

1. COSMIC, "2024 COSMIC Capstone Challenge – Information Packet," Baseline Document No: COSMIC-E01-WD001-2024-A, release date 7/10/2024, approved for unlimited public release. [Online]. Available: https://cosmicspace.org/c3.
2. Hitchens, T., "DARPA, spacelogistics step toward 2025 launch of orbital robotic 'mechanic' for Satellites," *Breaking Defense* Available: https://breakingdefense.com/2023/06/darpa-spacelogistics-step-toward-2025-launch-of-orbital-robotic-mechanic-for-satellites/
3. "Missions to hubble - NASA science," *NASA* Available: https://science.nasa.gov/mission/hubble/observatory/missions-to-hubble/.
4. J. R. Wertz and W. J. Larson, "Chapter 18: [Spacecraft Subsystems I - Propulsion]," in Space Mission Analysis and Design, 4th ed., J. R. Wertz, W. J. Larson, and D. R. Cichy, Eds. El Segundo, CA: Microcosm Press, 2018, pp. [534-538].
5. "Torayca® M60J," *Torayca® M60J (Carbon Fiber) by Troy: Technical Datasheet* Available: https://polymer-additives.specialchem.com/product/a-toray-torayca-m60j.
6. "How to connect batteries in series & parallel," *Power Sonic* Available: https://www.power-sonic.com/blog/how-to-connect-batteries-in-series-and-parallel/#:~:text=To%20configure%20batteries%20with%20a,with%20one%2012V%2020Ah%20battery.
7. "Spiral Coil Calculator," *Kaizer Power Electronics* Available: https://kaizerpowerelectronics.dk/calculators/spiral-coil-calculator/.
8. "Application data sheet: Mechanical properties of copper and copper alloys at low temperatures," *Standards & Properties: Mechanical Properties of Copper and Copper Alloys at Low Temperatures* Available: https://www.copper.org/resources/properties/144_8/.
9. Zhang, Z., and Pang, H., *Wireless Power Transfer: Principles and applications*, Hoboken, NJ, Piscataway, NY: John Wiley & Sons, Inc. ; IEEE Press, 2023.
10. Tsuruda, Y., *Introduction to CubeSat Power Control System* Available: https://www.unoosa.org/documents/pdf/psa/access2space4all/KiboCUBE/AcademySeason2/On-demand_Pre-recorded_Lectures/KiboCUBE_Academy_2021_OPL08.pdf.
11. J. R. Wertz and W. J. Larson, "Chapter 18: [Spacecraft Subsystems I - Propulsion]," in *Space Mission Analysis and Design*, 4th ed., J. R. Wertz, W. J. Larson, and D. R. Cichy, Eds. El Segundo, CA: Microcosm Press, 2018, pp. [534-538].
12. "CubeSat Form Factor Thermal Control Louvers | T2 Portal." *NASA* Available: https://technology.nasa.gov/patent/GSC-TOPS-40
13. "Multilayer Insulation Blankets | Aerospace Fabrication," *Aerospace Fabrication* Available: https://aerospacefab.com/products/multilayer-insulation/
14. SatCatalog. "CubeSat On-Board Computer." SatCatalog, [Online]. Available: https://www.satcatalog.com/component/cubesat-on-board-computer/ [Accessed: March 16, 2025].
15. Kuwahara, T. "Introduction to CubeSat Command and Data Handling System." *KiboCUBE Academy Lecture 10*, Tohoku University, [Online Presentation]. Available: https://www.unoosa.org/oosa/en/ourwork/psa/hsti/kibocube.html [Accessed: March 16, 2025].
16. "Metals Procurement Standards," *Blue Canyon Technologies* Available: https://www.bluecanyontech.com/static/datasheet/0DOC5161_RevB_Metals-Procurement-Standard.pdf.
17. "CUBESAT material limits for design for demise," *NASA* Available: https://ntrs.nasa.gov/api/citations/20140016958/downloads/20140016958.pdf.
18. Rocket Lab USA, Inc., "Payload User's Guide, Version 7.0," Rocket Lab USA, Inc., Nov. 2022. [Online]. Available: https://www.rocketlabusa.com/assets/Electron-Payload-User-Guide-7.0-v6.pdf. [Accessed: 8-Mar-2025].
19. "Aluminum 6061-T6; 6061-T651," *ASM material data sheet* Available: https://asm.matweb.com/search/specificmaterial.asp?bassnum=ma6061t6.
20. Blue Canyon Technologies, "Spacecraft," *Blue Canyon Technologies*. [Online]. Available: https://www.bluecanyontech.com/spacecraft.
21. Photovoltaics," *SEIA* Available: https://seia.org/photovoltaics/. [Accessed: Feb. 18, 2025]
22. "U.S. Energy Information Administration - EIA - independent statistics and analysis," *Photovoltaics and electricity - U.S. Energy Information Administration (EIA)* Available: https://www.eia.gov/energyexplained/solar/photovoltaics-and-electricity.php#:~:text=A%20photovoltaic%20(PV)%20cell%2C,or%20particles%20of%20solar%20energy. [Accessed: Mar. 01, 2025]
23. "Deployable Radiator - DCubed," *Dcubed* Available: https://dcubed.space/products/deployableradiator/
24. Nagano, H., Ohnishi, A., Higuchi, K., and Nagasaka, Y., "Experimental Investigation of a Passive Deployable/Stowable Radiator," *Journal of Spacecraft and Rockets*, Vol. 46, No. 1, 2009, pp. 185–190. https://doi.org/10.2514/1.30170
25. ResearchGate, "List of candidate ground stations," ResearchGate, [Online]. Available: https://www.researchgate.net/figure/List-of-candidate-ground-stations_tbl1_326072504. [Accessed: Mar. 16, 2025].
26. K. Heine, M. Ploner, and P. Gutjahr, "Earth and space observation at the German Antarctic Receiving Station O'Higgins," ResearchGate, Oct. 2014. [Online]. Available: https://www.researchgate.net/publication/266855813_Earth_and_space_observation_at_the_German_Antarctic_Receiving_Station_O'Higgins. [Accessed: Mar. 16, 2025].
27. Geological Survey, "The final journey of Landsat 5: A decommissioning story," Landsat Missions. [Online]. Available: https://www.usgs.gov/landsat-missions/final-journey-landsat-5-decommissioning-story. [Accessed: Mar. 9, 2025].